Lightweight Obstacle Detector Based on Scattered IR and Lock-In Filtering

B. Rosas-Flores, A. Hernández-Zavala, J. Huerta-Ruelas

PII: S1350-4495(19)30699-1
DOI: https://doi.org/10.1016/j.infrared.2019.103157
Reference: INFPHY 103157

To appear in: *Infrared Physics & Technology*

Received Date: 4 September 2019
Revised Date: 10 December 2019
Accepted Date: 10 December 2019

Please cite this article as: B. Rosas-Flores, A. Hernández-Zavala, J. Huerta-Ruelas, Lightweight Obstacle Detector Based on Scattered IR and Lock-In Filtering, *Infrared Physics & Technology* (2019), doi: https://doi.org/10.1016/j.infrared.2019.103157

Lightweight Obstacle Detector Based on Scattered IR and Lock-In Filtering

B. Rosas-Flores, A. Hernández-Zavala, J. Huerta-Ruelas

Instituto Politécnico Nacional, Centro de Investigación en Ciencia Aplicada y Tecnología Avanzada, Cerro Blanco 141 Colinas del Cimatario, Querétaro, México

Abstract

Obstacle detection in autonomous navigation involves the processing of the environment information obtained from sensors, such as LIDAR, radar, ultrasonic, magnetic and capacitive. Imaging techniques like stereoscopy, optical flux, and deep image, have been used for precise object detection but with a high computational cost. These sensors also have disadvantages like weight, its size or power consumption. The case of systems with lasers added like in LIDAR can be harmful to people. Ultrasonic sensors are safer for people but the signal to noise ratio decreases in outdoors. IR sensors are cheap and can be clustered to strength signal, however, additional sources of radiation can affect the measurement especially in outdoors. In this work, we propose an IR system with adequate spatial configuration and electronic filters to detect objects indoors and outdoors by means of scattered IR radiation centered at 940nm. The developed sensor has the following specs: Front area dimensions is 5x5 cm that includes 10 IR LEDs at the center and a Si detector in each corner. The approximated detection volume is 17,000 cm^3, considering a detection cone length of 300 cm and a solid angle of 30 degrees. Total system weight is 40 grams. System was tested with four experiments to evaluate signal filtering, effect of object surface roughness, repeatability and working sensitivity region. This evaluation allowed to make a comparison with traditional Obstacle Detection System techniques, giving advantages in almost all parameters considered, allowing us to conclude that developed system can detect objects in indoors and outdoors, in a region suitable for aerial and surface vehicles or blind persons.

Keywords— NIR Scattering, Lock-In Filter, Avoidance Sensor, Unmanned Vehicle, Obstacle detection

1. Introduction

Low-speed unmanned aerial and surface vehicles or sight aid technologies require lightweight and adequate sensors to avoid collisions. Important parameters like object distance, detection area, noise signal, sensor weight and system energy consumption must be considered in all navigation technologies. In drone applications, all these parameters reduce the effective time of flight or autonomy [1]. In the case of surface vehicles typically moving at low speed (<30km/h), they usually have dedicated activity in the same environment, such as agriculture [2]–[5]. In the case of sight aid technologies is very important a lightweight and discrete sensor to dissimulate the disability [6]–[9].

An Obstacle Detection System (ODS), is fundamental to prevent damage to any navigation platforms and its environment. In the case of Unmanned Aerial Vehicles (UAV), the market is growing exponentially. During 2017, the Federal Aviation Administration reported a registry of 670,000 drones only in the USA [10], contrasting with the sales report of one million units in the same year [11]. Unfortunately, they also reported 72 incidents involving aircrafts in February 2018 [12]. These numbers strongly suggest that it is required to include ODS in UAV's.

In case of surface vehicles, the applications are growing [3],[13], like swarm robots [14], monitoring [15] and services [2],[16], and even farming, are the most popular applications to avoid collisions. In the case of AID technologies for Visually Impaired People, they use light sensors in order to detect obstacles in normal navigation [17]. These sensors use audible or haptic feedback to inform about obstacles in the road. Most application use sensors mounted on gloves [9], shoes [8][18], sunglasses [7] and even cameras mounted in the chest. In these applications, the time of response is not critical due to the low speed of walking.

There is a linear relation between the information collected from sensors and the computational power required to process it. Image cameras are the most common solution to detect an object, however, the processing time with today´s technology is long for real-time detection using high definition images. Even the energy consumption and the computer resources required to process a high amount of data, requires specific hardware to process them, reducing system autonomy. LiDAR systems are precise and suitable for use mainly at outdoors, but they are limited by their size, weight, and energy consumption. In addition, they use concentrated and collimated laser radiation, harmful for working with humans around. There are infrared based detectors to determine the position of a vehicle within a controlled environment as in [19]-[20]. The

system uses an IR emitter and five detectors placed one in the center and one at each corner to determine an object distance. The intensity differences between detectors allows determining an absolute position, however, they require a special instrumented room, which limits their use at indoors. In the work [21], they use multiple IR sensors in the same vehicle to increase the resolution or the detection angle, but the system has limitations to work under direct sunlight. In [14], the sensor was placed on a mobile platform to swept the environment using a reduced number of sensors, generating a low density map and consequently the speed of the vehicle is reduced. Another technique that focuses in the processing of the signal with the objective of discarding false echoes for detecting true objects, is the use of ultrasonic spherical caps as in [22], but it does not work in outdoors. Other techniques use the time of flight of the signal, which considers the delay in traveling from the transmitter to the obstacle and back to the receiver as in [23]. A comparison between different sensor techniques used for obstacle detection in terms of the main descriptive parameters is give in section 2. Table 1, shows the status of obstacle detectors, helping to determine the need to develop other ODS to solve the current limitations.

In this work, we developed and tested an obstacle detector useful at indoors and outdoors scenarios. It is comprised of an array of IR receivers and filtering techniques for detecting the IR radiation scattered by the object to detect. System uses a Lock-in filtering technique to reject non-modulated IR signals, being capable of detecting only the modulated signal backscattered from the obstacle, working effectively at indoors and outdoors. The measured voltage intensity is related with the distance detection, having a maximum standard deviation of 5.8 percent, detecting the presence of objects in a range from 5 cm to 300 cm, in a 30° projection cone. At 3m distance, there is a circular projected detection area with a 1.5m diameter; i.e. for a 30cm vehicle, it represents five times its size. If a single laser is used as source, the probability of projecting the spot over the obstacle is weak, this is the reason to use multiple laser sweeps like in LiDAR systems, resulting in more weight, energy and computational costs. Systems based in cameras, have much more information and need to undistort the images to estimate the distance to an object.

The work is organized as follows: In section 2, it is described a quantitative and qualitative comparison between detection techniques to synthetize their characteristics and limitations. Section 3 describes the functioning of the MEOD (Minimal Element Object Detection) system. Section 4 presents the MEOD system performance validation through experiments that evaluates: signal stability in presence of an external source

of radiation (noise rejection); signal as function of surface angle/roughness and distance; Signal as function of surface angle/roughness and distance; repeatability and spatial performance as a function of distance/angle for a specific object. Section 5 presents the discussion that compares the developed MEOD system against current ODS.

2. Comparison between techniques to detect objects

From the literature review, we made a quantitative and qualitative comparison between systems and sensors, which is shown in Table 1. It synthetizes the following information: sensor type, Indoor and/or outdoor use, nominal distance, maximum speed, time response and application. A good ODS option for indoor use, are infrared sensors because they are cheap, easy to use and low weighted. In the presence of sunlight, this type of sensor does not work well without optical filters, since sunlight induces noisy signals.

Table 1: Comparison between different sensor techniques used for obstacle detection, in terms of main descriptive parameters

Sensor type	Indoor and/or Outdoor	Nominal Distance (m)	Maximum Speed	Time Response	Application
Cameras [2]	O	25	--	10 fps	Farm tractor
Lidar 16 [6]	I/O	--	60m/s	20 fps	Wheel chair
Ultrasonic [24]	--	0.3	slow	--	Surface
RGB-D [25]	I	--	500Hz	--	Quadcopter
LiDAR [23]	I	0.3	50 Hz	--	RoboBee
Velodyne [26]	O	2	10Hz	0.354 s	AGV
stereo [3]	O	--	15 Hz	37%	Boat
Cameras [27]	O	5 to 10	14 m/s	30 fps	Fix wing
IR cameras [28]	O	--	--	60 fps	Fix position

The relation between distance and recovered signal is represented in Figure 1. This graph compares the most used systems, such as LiDAR, Infra-Red (IR), Ultrasonic Sensor (US), Vision cameras, and our MEOD system; arranged by the distance range and detection area or field of view. A qualitative graphical representation using rectangular areas labelled with its technique name, give us an approximate view of traditional ODS performance. The intensity of any signal has an exponential decay behavior and is represented by the red line. The detection area is proportional to the distance represented by the black line, which turns into a discontinuous line while the signal intensity decreases. Our developed MEOD system provides a very useful operative region with better performance conditions than others do, as will be shown below.

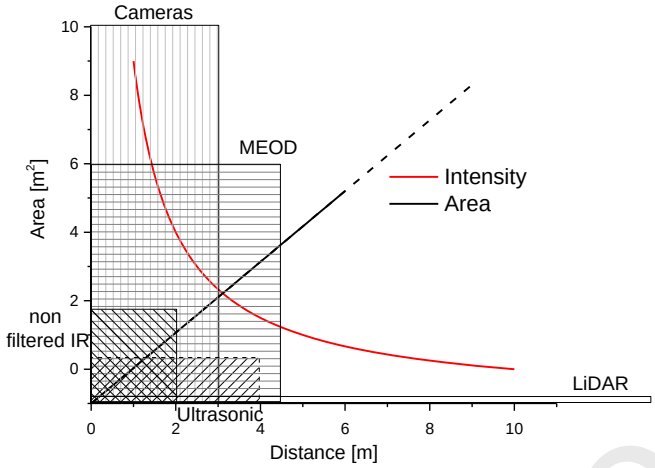

Figure 1. Work regions for most common obstacle detection techniques. Intensity of any signal has an exponential decay behavior and is represented by the red line. The detection area is proportional to distance represented by the black line which convert to a discontinuous line by signal intensity limitation.

3. SYSTEM DESCRIPTION

In this section, we present fundamental concepts about a generalized system based in scattered infrared radiation, the hardware configuration for the MEOD system developed, and the signal filtering strategy.

3.1. *Systems based in scattered infrared radiation for object detection*

An infrared emitter projects a characteristic non-visible cone of radiation within a numerical aperture defined in its specifications. When an object appears inside the volume of this cone of detection, a portion of the radiation is backscattered, which can be detected by the nearest IR detector, as shown in Figure 2.

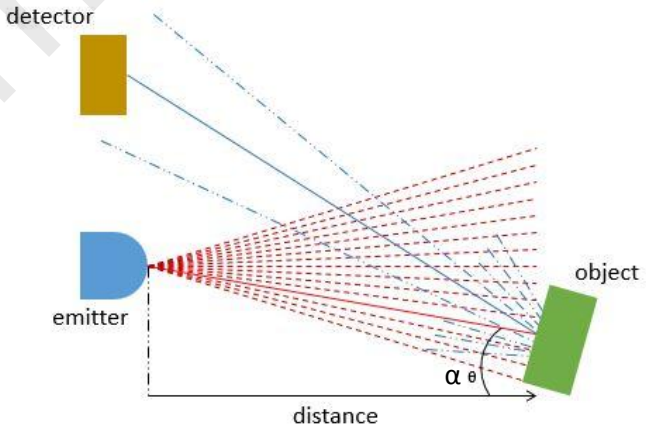

Figure 2. Optical system diagram showing the emitted radiation by the source represented with a cone on red dot lines, and the scattered radiation in blue dotted lines. The solid red line represents the average distance between the emitter and the object, while the solid blue line is the average distance between the object and sensor.

The detected signal depends on the object surface properties, and is proportional to the object size, and inversely proportional to the distance. Hence, it becomes necessary to include lenses to concentrate the weak scattered radiation.

3.2. *Hardware configuration (MEOD SYSTEM)*

The design of the MEOD system was bio-inspired by the eye evolution that started with an array of chromophore areas, which only sense changes in the intensity of radiation [22]. Since this primitive eye was very simple, it had to evolve, with a relation between brainpower and eye resolution. As a comparison, an HD camera requires bigger computational capabilities than a VGA one. For that reason, we chose to use a small detector array (4 lens/detector sets) and efficient filters to provide a similar response with less data. The lenses have a focal distance of 9mm, with a diameter of 10mm, and are placed at the top of each receiver, as shown in Figure 3.

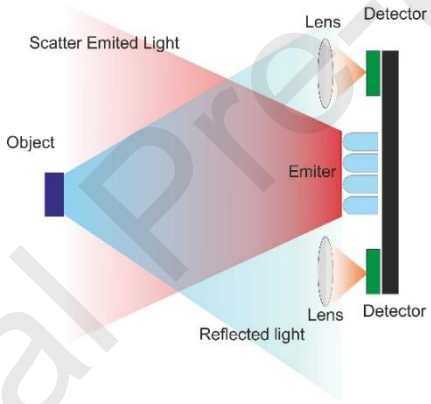

Figure 3 MEOD system sketch. The radiation cone is represented in red and scattered radiation from the object in blue. The detectors are the green boxes and the concentrated scattered radiation is the small orange cones drawn between lens and detectors.

The MEOD system was designed to have a field of view like ordinary cameras but with a small amount of detection data points. Our system integrates the entire detected signal backscattered in a lens area in just one detector. The four sensors contribute with a portion of this signal, which is processed by the filter, generating an analog signal corresponding to object to be detected. Each detector has 2.4 x 2.4 mm detection area, with 70 degrees solid angle detection [29]. If it is required to increase the detection distance, a bigger array of emitters can increase the intensity of the emitted radiation and directly the scattered radiation.

The physical configuration of the detector array is shown in Figure 3-a. Each detector perceives slightly different information about the scene. They are located at the four corners (white circles) and the array of

emitters is placed at the center (red circles). This array allows increasing the signal-to-noise ratio by analyzing the four signals. The measurement of each detector is processed and compared with the others, to obtain information about the presence of the obstacle around the vehicle path.

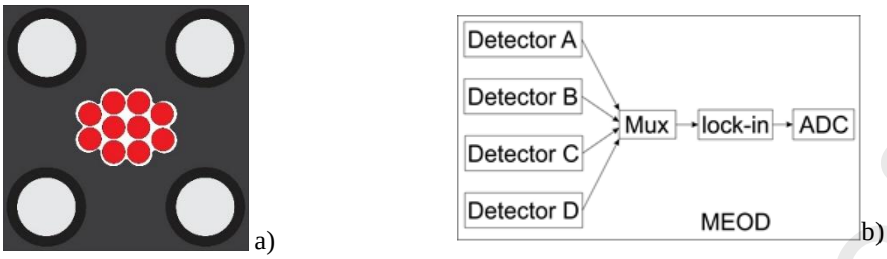

Figure 3. a) System case. The detectors are at the four corners and the array of 10 emitters is placed at the center. b) Block diagram of the MEOD system, the signal of each detector is multiplexed and processed by a PSD filter to reject the noise.

The MEOD system works based on the intensity of a modulated emitted radiation, which travels freely until it reaches the surface of an object that scatters it in different directions according to its properties. The four detectors receive a fraction of this radiation, whose back-scattered intensity is given by:

$$I \propto \frac{1}{2d^2} \tag{4}$$

where *I* correspond to the intensity of the emitted radiation and *d* is the average distance between the radiation source and the object surface; note that the radiation travels two times the same distance, as illustrated in Figure 2. The distance can be expressed in terms of a radius *r* as

$$r = \frac{d}{cos\alpha} \tag{5}$$

where α represents the position angle of the obstacle with respect to the MEOD system. The scattering of this radiation is affected by the geometric and surface properties of the objects. Additionally, solar radiation generates an offset that increases the detection voltage and must be filtered.

3.3. *Signal filtering for scattered radiation detection*

In order to filter the signal, the MEOD system includes a Phase Sensitive Detector (PSD), using a Lock-in filter for discriminating non-pulsed sources of IR radiation such as the sunlight and lamps [29]. The block diagram in Figure 3-b, shows the four detectors, the multiplexer and the lock-in filter. To reduce the number of electronic components, the output of each detector is multiplexed to use just one lock-in filter circuit (AD630 from Analog Devices) [30], which results in less weight and lower energy consumption. If the detected frequency is equal to the source, the convolution maximizes its value [31], and in any other case the

result tends to zero. The output voltage V_o, is the multiplication of two sine waves, the signal reference and the detected signal.

$$V_o = \mathrm{Asin}(\omega t)\ 1/2 V_{sig} V_L \cos(\theta_{sig} - \theta_{ref}) \quad (7)$$

where V_{sig} is the reference signal and V_L is the detected signal, $\theta_{sig} - \theta_{ref}$ is the phase between signals.

The optimal frequency was determined by scanning the frequencies from 100Hz to 1Khz. An optimum modulation frequency of 550Hz was determined after the sweep test, finding at this frequency the best signal-to-noise ratio with attenuation noise of 20.6dB obtained with the formula [32]:

$$SNR = 10\ Log_{10}\ (s/n) \quad (8)$$

4. System performance validation

MEOD system uses scattered IR radiation in order to detect objects within the projection volume, which behaves like a cone that grows with the distance. The minimum detection transversal area corresponds to 10 cm distance, generating a rounded spot area of 22cm^2 (5.3cm diameter) and the maximum detection transversal distance is at 300cm projecting an approximate spot area of 20000cm^2 (160cm diameter). To validate the system, four different experiments were performed. The first experiment was designed to evaluate noise rejection performance with an intermittent noise source. The second one was to evaluate the distance effect for different roughness surfaces. The third one was to evaluate the system repetitiveness, and the last experiment was to evaluate the backscattered signal from a specific object, as function of distance and angle with respect to the MEOD sensor position. These experiments are described in the following sections.

4.1. *MEOD signal with different ambient radiation intensity*

The integrated sensor signal obtained after the signal/reference convolution is affected by attenuating factors like surface roughness or scattered angle that changes the intensity of the detected scattered radiation. To determine the attenuation as a function of the angle and the object surface roughness, three glasses of 15 cm x 15 cm were used to form a pentahedron with triangular base as shown in Figure 4. This pentahedron is mounted on a rotating platform with an encoder of 6000 pulses per revolution. The surfaces selected for testing are: stipolite glass, sandblasted glass and glossy black film. To evaluate the disturbance generated by an external signal source, we used a led lamp modulated at 2Hz with a luminous intensity of 71 lux at a 120 cm distance. Average ambient illumination was 30 lux. The surface roughness affects the distribution of the signal. As an example, in case of specular texture, the signal is detected only when the surface is

perpendicular to incidence radiation.

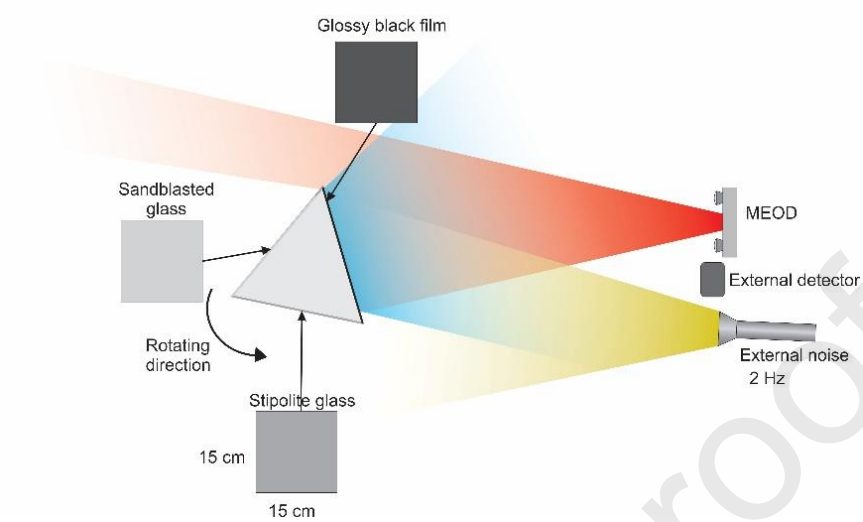

Figure 4. Experimental setup with a rotating polyhedron to validate the system with different surface roughness. It includes a lamp modulated at different frequency as a perturbation source to evaluate filter performance.

The experiment consists with the projection of the IR radiation over the pentahedron under rotation, adding a interference of a lamp modulated at different frequency during a second revolution, as shown in Figure 5. The red plot shows the signal after two complete revolutions and the black plot is a signal from an auxiliary detector to monitor the complete ambient radiation. Signal filtered by MEOD changes only 4.2% with respect to the signal without perturbation, presenting a positive filtering performance.

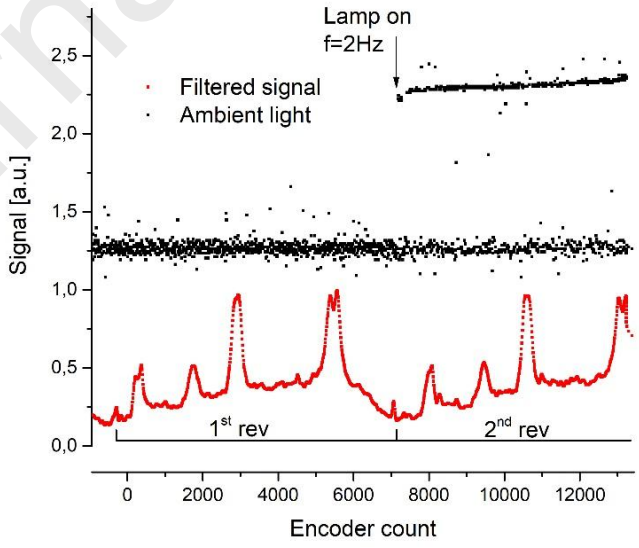

Figure 5. MEOD signal after two revolutions with and without an external perturbation lamp. The red plot is the MEOD signal, and the black plot is the signal from environmental light present during the experiment.

After the lamp is turned on, it is seen that the external detector signal in black increases, with no considerable change in the MEOD signal.

4.2. *Signal as a function of surface angle/roughness and distance*

To determine sensor sensitivity as a function of surface roughness, distance and incidence angle, four different surfaces were tested. The tested surfaces selected were: stipolite glass, sandblasted glass, glossy black film and black matte paper (black matte paper was added at stipolite glass position after this was measured). The experiments were made at different distances from MEOD system to the polyhedron {80, 120, 170, 260} cm, as in Figure 6. It could be observed that signal peaks correspond when the object surface is perpendicular to the incidence radiation. FWHM peak values are dependent in surface roughness and maximum intensity is inversely proportional to the object distance.

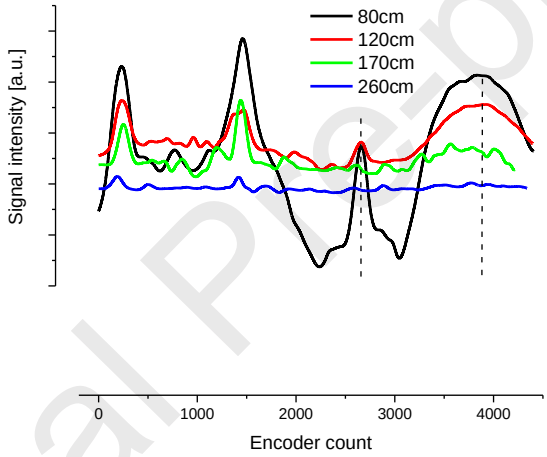

Figure 6. Comparison of signal intensities as function of incidence angle (proportional to encoder counts), at four different object distances (80, 120, 170 and 260 cm). Signal peaks correspond when a surface is perpendicular to incidence radiation. FWHM peak values are dependent in surface roughness and maximum intensity is inversely proportional to object distance.

4.3. *Repeatability*

To evaluate repeatability, data from five revolutions were obtained with the experimental setup showed in Figure 4, and divided into five data sets, which are plotted together in Figure 7. In this experiment similar environmental conditions were kept for all measurements with the pentahedron rotating at a velocity of 200 encoder pulses by second. The intensity levels for each peak, corresponding to stipolite glass, sandblasted glass and glossy black film are reproduceable with a slight variation when the angle is not perpendicular to the incidence direction of infrared radiation. After a statistical analysis a maximum error of 4% and a standard deviation of 0.043 was obtained.

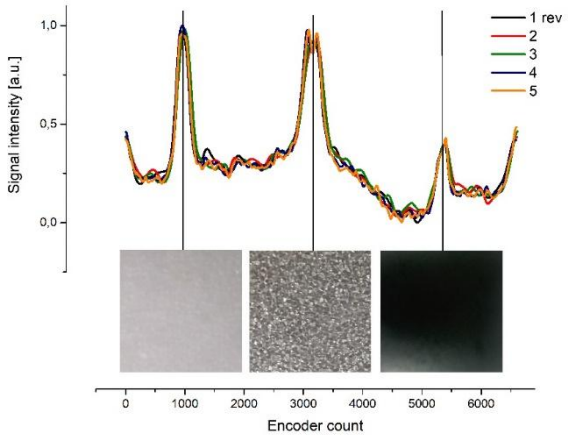

Figure 7. Repeatability of signal intensity during 5 revolutions as a function of encoder count (angle) for stipolite glass, sandblasted glass and glossy black film.

4.4. *Spatial performance as a function of distance and angle for a specific object*

In the fourth experiment, to determine the resolution and the maximum detection angle, the sensor was moved to different places in a 160x300cm *XY* plane. A block of black rough foam with high contrast was used as an obstacle with reflective tape in the center. A coordinate machine was employed to move the object and get precision in the positions and repeatability on the measurements. The position mesh was divided into three regions as a function of distance (15-120cm, 120-210cm, 210-300cm). The regions have 160, 60 and 42 points respectively. The MEOD system acquired 16 samples per detector at each position. The plot in Figure 8, illustrates the different intensities for each measurement in an environment using a black rugged obstacle and 1600 lux of ambient light, notice that these settings were defined to approximate the system to potential noisy conditions. The maximum signal intensity for these conditions is around a distance of 180cm. In outdoor environmental conditions, the MEOD can detect the presence of an obstacle up to 3m.

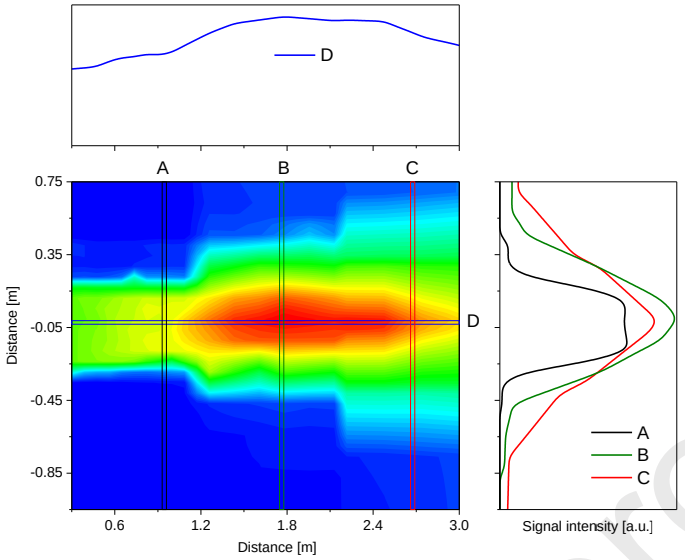

Figure 8. Output voltage generated by the MEOD system using a mesh with three zones. The points are separated into three regions: 15-120cm, 120-210cm, 210-300cm. Plot at the right side shows the signal intensity at three different cross sections; line labeled A correspond to closer points, line B include the maximum value on intensity on the middle region, and line C is at the farthest region showing the signal decay. The upper plot corresponds with intensity signal along the central line.

5. DISCUSSION

The MEOD system was tested in different environment conditions. The optimal frequency was determined by swapping the modulation signal, obtaining the maximal response at 550Hz. A perturbation was added on the measured signal to validate the efficiency of the filtering process. The intensity signal at different distances and roughness surfaces is consistent in all the experiments. The statistical analysis of data from different experiments to evaluate repeatability showed a 4.2% variation, which is considered acceptable for object detection. Finally, we created a mesh with the intensity signal points on three regions, with increasing distances in typical environment conditions. This distribution of measured points allows to determine the optimum operation region and its boundaries. If an object is 10 cm close, this radiation will be more intense than when the object is as far as 300 cm or there is no object in the scene.

There are critical cases in which the MEOD system could fail, such as sunrise and dawn, especially when the MEOD is facing directly to the sun. It is in that instant when the intensity of the sunlight saturates the detectors leading to signal loss. Another issue that blinds the MEOD system, is when trying to detect objects with a specular surface. In these cases, the scatter becomes so weak that the MEOD system only detects it when it is close enough to the sensor. In the experimentation to validate the system, MEOD was able to detect

different finishing materials; however, the output strongly depends on the surface roughness.

In the following, we provide a quantitative and qualitative comparison between tested MEOD system against other detection most available commercial technologies. Figure 9 shows the experimental setup used to compare MEOD with five different type of sensors: a LiDAR Scanse Sweep v1.0, a sonar EZ1/ B1210, an effect doppler radar Doradus HB100, a vision camera model Q2F-00009 and an infrared sensor 2Y0A02. All sensors were fixed in a base close to each other, in front of a mobile object (white square foam with 15cm sides), motorized to get a speed control in a 200cm path. The issues considered are field of view (FOV), indoor/outdoor operation, feedback control type signal, weight, energy consumption, cost and existence of a noise rejection filter. Experiments were performed at three distances 80, 120 and 300 cm, as the calibration experiments previously described.

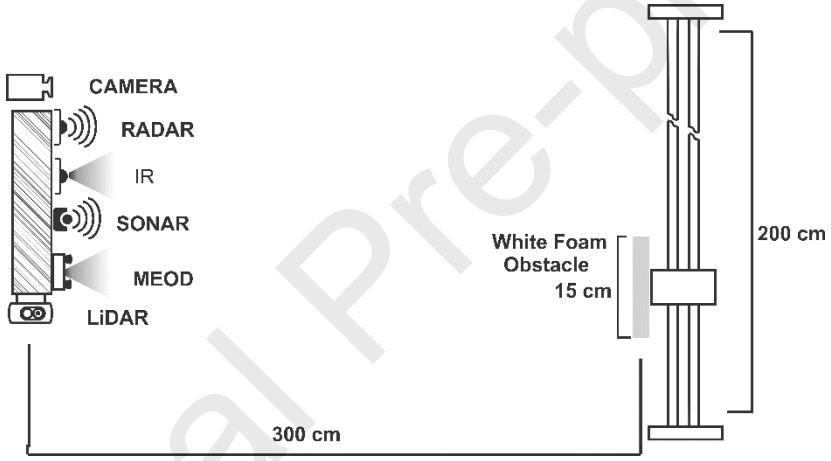

Figure 9. Experimental setup to compare MEOD system with low weight and low cost commercial available sensors traditionally used to detect obstacles.

The MEOD system uses modulated IR radiation, and filtering techniques to recover the signal. This is the main difference with the normal IR systems such as in [33], and the increase of weight is comparative with a composite sensor [34] providing more distance range, and a similar range is obtained with less weight [35]. A broad angle of detection generates a bigger sweep area which increases the probability of detecting an obstacle in comparison with a laser system that needs to sweep mechanically the spot at higher frequencies to increase the detection probability. In the case of ultrasound, the environment affects the measurement because signal absorption increases in a structured environment. Nevertheless, we can detect objects in low visibility conditions such as fog or smoke. In the case of radar systems, they depend on conductivity to detect an obstacle; this is a problem with obstacles such as non-conductive obstacles. The MEOD system uses a single

analog feedback signal, allowing fast information processing which can increase the speed of the vehicle. In contrast with image processing, that depends on image resolution and the hardware computational power. Comparison results are summarized in Table 2.

Table 2. MEOD system comparison considering most important parameters, against current technologies for obstacle detection.

	Technique / Model					
Property	LiDAR Scanse sweep 1.0	Sonar EZ1 / Mb 1210	Radar Doradus HB100	Camera Q2F-00009	IR 2Y0A02	MEOD
Field of View (degrees)	360	30	40	60	15	30
Time to process (ms)	6500	20	30	250	15	20
Moving parts	Yes	No	No	No	No	No
Outdoors	Yes	Yes	Yes	No	No	Yes
Feedback Control signal type	Cloud Points	Analog	Analog	Matrix of values	Analog	Analog
Weight (grs)	400	20	30	50	15	45
Energy consumption (mW)	1500	100	200	750	175	600
Cost (US$)	500	13	8	47	15	35
Active sensor with high noise rejection filter	Yes	No	No	No	No	Yes

6. CONCLUSION

This work uses the scattered IR signal, to determine the presence of an obstacle on the route of a lightweight vehicle or a blind person. This system allows detecting objects in a wide projection area generated by IR radiation sources. The weak scattered signal by an object is concentrated on the sensors by the use of lenses, filtered and amplified with an analog sensitive phase lock-in detector with a high noise rejection performance, allowing to detect a enough quantity of scattered radiation to avoid them.

MEOD system was tested with four experiments to evaluate signal filtering, effect of object surface roughness, repeatability and operating region. Additionally a quantitative and qualitative comparison was performed with five traditional ODS techniques, obtaining advantages in most of parameters considered (weight, energy consumption, cost, FOV, Time to process, feedback control), allowing us to conclude that the developed MEOD system can detect objects at indoors and outdoors, in a suitable region for aerial and surface vehicles, or blind persons.

ACKNOWLEDGMENTS

Authors would like to thank to the Centro de Investigación en Ciencia Aplicada y Tecnología Avanzada, from the Instituto Politecnico Nacional in Querétaro México, and to the Consejo Nacional de Ciencia y Tecnología (CONACYT) México, for their support in the realization of this work.

REFERENCES

[1] N. Gageik, P. Benz, and S. Montenegro, "Obstacle Detection and Collision Avoidance for a UAV with Complementary Low-Cost Sensors," *IEEE Access*, vol. 3536, no. c, p. 1, 2015.

[2] T. Korthals, M. Kragh, P. Christiansen, H. Karstoft, R. N. Jørgensen, and U. Rückert, "Multi-Modal Detection and Mapping of Static and Dynamic Obstacles in Agriculture for Process Evaluation," *Front. Robot. AI*, vol. 5, no. March, 2018.

[3] B. Bovcon, R. Mandeljc, J. Perš, and M. Kristan, "Stereo obstacle detection for unmanned surface vehicles by IMU-assisted semantic segmentation," *Rob. Auton. Syst.*, vol. 104, pp. 1–13, 2018.

[4] Z. Yang, Z. Fang, and P. Li, "Bio-inspired Collision-free 4D Trajectory Generation for UAVs Using Tau Strategy," *J. Bionic Eng.*, vol. 13, no. 1, pp. 84–97, Jan. 2016.

[5] K. Harikumar, T. Bera, R. Bardhan, and S. Sundaram, "Autonomous navigation and sensorless obstacle avoidance for UGV with environment information from UAV," *Proc. - 2nd IEEE Int. Conf. Robot. Comput. IRC 2018*, vol. 2018-Janua, no. 1, pp. 266–269, 2018.

[6] R. Arnay, J. Hernandez-Aceituno, J. Toledo, and L. Acosta, "Laser and Optical Flow Fusion for a Non-Intrusive Obstacle Detection System on an Intelligent Wheelchair," *IEEE Sens. J.*, vol. 18, no. 9, pp. 3799–3805, 2018.

[7] J. Bai, Z. Liu, Y. Lin, Y. Li, S. Lian, and D. Liu, "Wearable Travel Aid for Environment Perception and Navigation of Visually Impaired People," pp. 1–7, 2019.

[8] K. Patil, Q. Jawadwala, and F. C. Shu, "Design and Construction of Electronic Aid for Visually Impaired People," *IEEE Trans. Human-Machine Syst.*, vol. 48, no. 2, pp. 172–182, 2018.

[9] S. Jain, D. Sushanth, V. N. Bhat, and J. V Alamelu, "Design and Implementation of the Smart Glove to Aid the Visually Impaired," *2019 Int. Conf. Commun. Signal Process.*, pp. 662–666, 2019.

[10] "State and County Inquiry." FAA registry.

[11] "drones sales March 21, 2017." FAA sales.

[12] "Preliminary Accident and Incident Reports." FAA incident.

[13] H. Zhang, W. Tao, J. Huang, and R. Zheng, "Development of An In-building Transport Robot for Autonomous Usage of Elevators," *2018 Int. Conf. Intell. Saf. Robot. ISR 2018*, pp. 44–49, 2018.

[14] G. Lee and N. Y. Chong, “Low-cost dual rotating infrared sensor for mobile robot swarm applications,” *IEEE Trans. Ind. Informatics*, vol. 7, no. 2, pp. 277–286, 2011.

[15] N. Karapetyan, J. Moulton, J. S. Lewis, A. Quattrini Li, J. M. Okane, and I. Rekleitis, “Multi-robot Dubins Coverage with Autonomous Surface Vehicles,” *Proc. - IEEE Int. Conf. Robot. Autom.*, pp. 2373–2379, 2018.

[16] N. Jeong, H. Hwang, and E. T. Matson, “Evaluation of low-cost LiDAR sensor for application in indoor UAV navigation,” *2018 IEEE Sensors Appl. Symp. SAS 2018 - Proc.*, vol. 2018-Janua, no. Figure 1, pp. 1–5, 2018.

[17] R. Jafri, R. L. Campos, S. A. Ali, and H. R. Arabnia, “Visual and infrared sensor data-based obstacle detection for the visually impaired using the Google Project Tango Tablet development kit and the unity engine,” *IEEE Access*, vol. 6, pp. 443–454, 2018.

[18] T. Lin, C. Yang, and W. Shih, “Fall Prevention Shoes Using Camera-Based Line-Laser Obstacle Detection System,” *J. Healthc. Eng.*, vol. 2017, pp. 1–11, 2017.

[19] E. M. Gorostiza, J. L. Lázaro Galilea, F. J. Meca Meca, D. Salido Monzú, F. Espinosa Zapata, and L. Pallarés Puerto, “Infrared sensor system for mobile-robot positioning in intelligent spaces,” *Sensors*, vol. 11, no. 5, pp. 5416–5438, 2011.

[20] D. Yang, B. Xu, K. Rao, and W. Sheng, “Passive Infrared (PIR)-Based Indoor Position Tracking for Smart Homes Using Accessibility Maps and A-Star Algorithm,” *Sensors*, vol. 18, no. 2, p. 332, 2018.

[21] P. M. Novotny and N. J. Ferrier, “Using infrared sensors and the Phong illumination model to measure distances,” in *Robotics and Automation, 1999. Proceedings. 1999 IEEE International Conference on*, 1999, vol. 2, pp. 1644–1649.

[22] F. T. Moreno-Ortiz, E. Castillo-Castaneda, and A. Hernandez-Zavala, “Detection and location of surfaces in a 3D environment through a single transducer and ultrasonic spherical caps,” *Ing. E Investig.*, vol. 37, no. 3, pp. 37–44, 2017.

[23] E. F. Helbling, S. B. Fuller, and R. J. Wood, “Altitude Estimation and Control of an Insect-Scale Robot with an Onboard Proximity Sensor,” in *Robotics Research*, Springer, 2018, pp. 57–69.

[24] B. S. Lim, S. L. Keoh, and V. L. L. Thing, “Autonomous vehicle ultrasonic sensor vulnerability and impact assessment,” *IEEE World Forum Internet Things, WF-IoT 2018 - Proc.*, vol. 2018-Janua, pp. 231–236, 2018.

[25] M. Odelga, P. Stegagno, N. Kochanek, and H. H. Bülthoff, “A Self-contained Teleoperated Quadrotor : On-board State-Estimation and Indoor Obstacle Avoidance,” pp. 7840–7847, 2018.

[26] Z. Rozsa and T. Sziranyi, “Obstacle prediction for automated guided vehicles based on point clouds measured by a tilted lidar sensor,” *IEEE Trans. Intell. Transp. Syst.*, vol. 19, no. 8, pp. 2708–2720, 2018.

[27] A. J. Barry, P. R. Florence, and R. Tedrake, “High-speed autonomous obstacle avoidance with pushbroom stereo,” *J. F. Robot.*, vol. 35, no. 1, pp. 52–68, 2018.

[28] Y. Liu and R. Bucknall, “Path planning algorithm for unmanned surface vehicle formations in

a practical maritime environment," *Ocean Eng.*, vol. 97, pp. 126–144, Mar. 2015.

[29] S. Martini *et al.*, "Distributed motion misbehavior detection in teams of heterogeneous aerial robots," *Rob. Auton. Syst.*, vol. 74, pp. 30–39, Dec. 2015.

[30] D. ANALOG, *Balanced Modulator AD630*, Reb G. MA 02062-9106, U.S.A.: Analog Devices, Inc, 2016.

[31] Q. Tang *et al.*, "Detection of Weak Near-Infrared Signal Based on Digital Orthogonal Vector Lock-in Amplifier," pp. 2–4.

[32] J. R. Raol, *Multi-sensor data fusion with MATLAB*. CRC press, 2009.

[33] N. Gageik, P. Benz, and S. Montenegro, "Obstacle Detection and Collision Avoidance for a UAV with Complementary Low-Cost Sensors," *IEEE Access*, vol. 3536, no. c, p. 1, 2015.

[34] Z. Dengtao, Z. Yan, L. Ruigang, and L. Jianlin, "MULTI-SENSOR FUSION BASED UAV COLLISION AVOIDANCE SYSTEM," *J. Teknol.*, vol. 2005, pp. 105–106, 2005.

[35] Q. Zhou, D. Zou, and P. Liu, "Hybrid obstacle avoidance system with vision and ultrasonic sensors for multi-rotor MAVs," *Ind. Rob.*, vol. 45, no. 2, pp. 227–236, 2018.

Highlights

New sensor with IR emitters for obstacle detection in lightweight systems.

Active sensors include PSD filtering with a continuous analog feedback signal.

Low cost and lightweight sensor that operates with better eye-safe operation.

Sensor added in a mobile entity allows to detect obstacles in indoors/outdoors.